Design and Implementation of a Linear Quadratic Regulator Based Maximum Power Point Tracker for Solar Photo-Voltaic System

D. S. Karanjkar[1], S. Chatterji[1] and Amod Kumar[2]

[1]Electrical Department, National Institute of Technical Teachers Training and Research, Chandigarh, India
[2]Central Scientific Instruments Organization, Chandigarh, India

karanjkards@gmail.com, chatterjis@yahoo.com, amod.csio@yahoo.com

Abstract

A maximum power point tracking (MPPT) technique based on linear quadratic regulator (LQR) approach for solar photo-voltaic system has been proposed in this paper. LQR based MPPT controller has been designed with online set-point adjustment approach using current, radiation and temperature sensors. Real time simulations have been carried out on MATLAB^{TM}/dSPACE^{TM} platform for solar photo-voltaic system with buck converter. Performance of the proposed technique hase been compared with perturb and observe, incremental conductance, fuzzy logic, neural network and ANFIS based methods of maximum power point tracking. Experimental results showed the superiority of the proposed method for tracking maximum power point under rapidly varying solar radiations.

Keywords: *Maximum power point tracking; solar photo-voltaic system; linear quadratic regulator*

1. Introduction

Solar energy is clean, abundant, renewable and freely available source of the energy. The major obstacle for the penetration and reach of solar photo-voltaic (PV) systems is their low efficiency and high capital cost. The output voltage of the PV system is highly dependent on solar irradiance and panel temperature. The maximum power point tracking (MPPT) system is necessary to ensure the maximum power generation. Perturb and observe (P&O), incremental conductance (INC), fuzzy logic, neural network (NN), adaptive neuro-fuzzy inference system (ANFIS) and current / voltage feedback based techniques are few of many available MPPT methods [1]. Out of most widely used MPPT techniques, incremental conductance and artificial intelligence based techniques have higher accuracy but they are complex in design. P&O technique having moderate accuracy is the most extensively used in commercial MPPT systems [2]. With this approach oscillation are developed around the desired operating point which causes power loss. As compared to P&O technique, voltage / current feedback technique is a simple technique in which the feedback of panel voltage or current is taken and compared with a pre-calculated reference voltage or current; the duty-ratio of dc-dc converter is continuously adjusted so that it operates close to that of maximum power point (MPP) [1]. Due to pre-calculated constant reference voltage/current it cannot track MPP during changing environmental conditions [3].

Linear quadratic regulator (LQR) is one of the methods of optimal control strategy which has been widely developed and used in various applications. LQR design is based on the selection of feedback gain such that the cost function *J* is minimized [9]. In this paper LQR

based controller has been designed with dynamic set-point adjusting approach without need of power calculation. Performance of the proposed techniques has been compared with existing MPPT methods. The paper has been organized as follows: Design aspects of proposed MPPT controllers have been described in section two. Real time implementation of proposed and existing MPPT techniques on MATLAB^{TM}/dSPACE^{TM} platform has been described in section three. Experimental results and comparison of proposed and existing MPPT techniques have been given in section four. In the fifth section conclusions have been discussed.

2. Proposed MPPT Controllers

Solar system with buck converter (Figure 1(a)) has been considered in the present work. The output voltage of the buck converter is regulated by changing duty-ratio of the semiconductor switch. When the switch is *on*, the diode is reverse biased, the inductor and the load gets energy from the input solar energy. During *off* state of the switch the diode gets forward biased and the output stage receives the energy from the inductor and the input remains isolated. The net energy transferred to the output from input is always lesser than that of input in given switching cycle. The ratio of output to input voltage is called as the duty-ratio (*D*) and can also defined as the ratio of the *on* time of the switch to the total switching period [10].
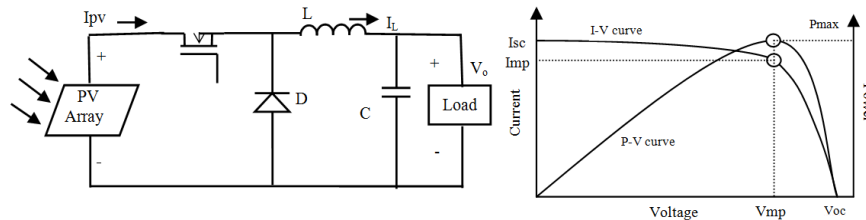

Figure 1. (a) Configuration of buck converter in solar PV system and (b) *I-V* and *P-V* characteristics of a solar cell

Current-voltage (*I-V*) and power-voltage (*P-V*) characteristics of a typical solar cell, at a fixed ambient temperature and solar irradiation are non-linear in nature and shown in Figure 1(b). The span of the *I-V* curve ranges from the short-circuit current (I_{sc}) to open-circuit voltage (V_{oc}). At the 'knee' of a normal *I-V* curve is the maximum power point (I_{mp}, V_{mp}), the point at which the PV cell generates maximum electrical power [4]. The block diagram of conventional current feedback MPPT system has been shown in Figure 2(a) [1]. Although this technique uses only current sensor it cannot track maximum power point during changing environmental conditions due to pre-calculated constant reference current. Proposed LQR and LQR-PI MPPT Control techniques include online set-point adjustment approach based on actual radiation and temperature values. The block diagram of the proposed approach has been shown in Figure 2(b).

2.1 Design of set-point tracker

The mathematical expression of the output current of the PV module (Figure 2) can be expressed as [4]:
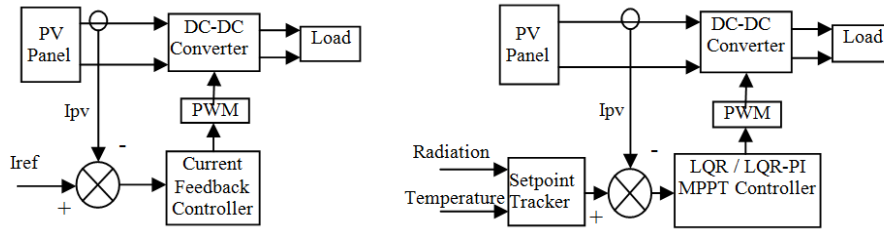
Figure 2. (a) Current feedback MPPT control scheme and (b) Block diagram of proposed control schemes for MPPT

$$I = I_{pv}n_p - I_o n_p \left[\exp\left(\frac{V + R_s I}{V_t a}\right) - 1 \right] - \frac{V + R_s I}{R_s} \tag{1}$$

where, I is the current, V is the voltage of the PV module, I_{pv} is the photo-current, I_0 is the reverse saturation current, n_p is the number of cells connected in parallel, n_s is the number of cells connected in series, q is the charge of an electron ($1.6*10^{-19}$C), k is Boltzmann's constant ($1.38*10^{-23}$J/K), a is p-n junction ideality factor, ($1 < a < 2$, $a = 1$ being the ideal value), and T is the PV module temperature. R_s and R_p are equivalent series and parallel resistances. The thermal voltage of the module with N_s cells connected in series is denoted by $V_t = N_s kT /q$. The assumption $I_{sc} \approx I_{pv}$ has mostly been used in photovoltaic models because in practical devices the series resistance is low and the parallel resistance is of high value. The PV current depends on the solar irradiation and is influenced by the temperature according to the following equation,

$$I_{pv} = (I_{pv,n} + K_I (T - T_n)) \frac{S}{S_n} \tag{2}$$

where $I_{pv,n}$ is the PV current at the nominal condition (at 25 ^{0}C and 1000W/m^2), T and T_n are the actual and nominal temperatures, S and S_n are actual and nominal radiation and the short-circuit current/temperature coefficient (K_I). Diode saturation current depends on the solar radiation and the temperature as:

$$I_0 = I_{0,n} \left[\frac{T_n}{T}\right]^3 \exp\left(\frac{qE_g}{ka}\left[\frac{1}{T_n} - \frac{1}{T}\right]\right) \tag{3}$$

where, E_g is the band-gap energy of the semiconductor and $I_{0,n}$ is the nominal saturation current given by,

$$I_{0,n} = \frac{I_{sc,n}}{\exp\left(\frac{V_{oc,n}}{aV_{t,n}}\right) - 1} \tag{4}$$

with $V_{t,n}$ being the thermal voltage at the nominal temperature T_n and $I_{sc,n}$ is the short-circuit current at the nominal condition. Short-circuit current I_{sc} of the PV module is not strongly temperature dependent it tends to increase slightly with increase of the module temperature. For the purpose of experimental comparison of various MPPT algorithms variation in short-circuit current with change in temperature can be considered negligible. The short-circuit current then can be determined by,

$$I_{sc} = I_{sc,n} \left(\frac{S}{S_n} \right)^{\alpha} \tag{5}$$

where, I_{sc} is the short-circuit current of the PV module under the irradiance S; α is the exponent responsible for all the non-linear effects that the photocurrent depends on. Under different irradiance levels, short-circuit current is different, so that the parameter α can be determined by:

$$\alpha = \frac{\ln \left(I_{sc,n} / I_{sc,1} \right)}{\ln \left(S_n / S_1 \right)} \tag{6}$$

where $I_{sc,n}$ and $I_{sc,1}$ are the short-circuit currents of the PV module under radiation S_n and S_1. The relation between I_{sc} and I_{mp} can be given by,

$$I_{mp} = k \times I_{sc} \tag{7}$$

where, the factor k is always <1 and k varies from between 0.78 and 0.92 and the common value of k is 0.9 [5]. Measuring I_{sc} during operation is difficult and hence in the present work I_{sc} is determined based on equation (5) & (6). Values of $I_{sc,1}$ and S_1 are referred from the *I-V* curves provided in the manufacturer's datasheet. Set-point tracking algorithm has been designed based on equations (5), (6) and (7). Dynamic set-point tracking assures the dynamic operating point of the proposed controllers at current at maximum power point (*Imp*).

2.2 Design of LQR based MPPT system

The term "linear quadratic" refers to the linear system dynamics and the quadratic cost function. LQR design is based on the selection of feedback gain such that the cost function J is minimized [9]. This ensures that the gain selection is optimal for the cost function specified. For LQR design the system need to be described by state space model:

$$\dot{x} = Ax + Bu \tag{8}$$

$$y = Cx + Du \tag{9}$$

The performance index is defined as,

$$J = \int_0^{\infty} \left(x^T Q x + u^T R u \right) dt \tag{10}$$

where, Q and R are the weight matrices. Q is positive definite or positive semi-definite real symmetric matrix and R is positive definite symmetric matrix. The feedback control function limits to a linear function so that,

$$u = -Kx \tag{11}$$

where, K is given by,

$$K = R^{-1} B^T P \tag{12}$$

and P can be determined by solving the continuous time algebraic *Riccati* equation,

$$A^T P + PA - PBR^{-1} B^T P + Q = 0 \tag{13}$$

The advantage of using the quadratic optimal control scheme is that the system designed will be stable and robust, except in the case where the system is not controllable. In order to design LQR and LQR-PI MPPT controllers small signal model of the buck converter has been considered in the present work. Overall transfer function model of buck converter in current programmed mode is shown in Figure 3 [12]. The small *ac* variations in output voltage and inductor current can be expressed via superposition as a function of small *ac* variations in duty-ratio and the input voltage and by defining transfer functions $G_{vd}(s)$, $G_{id}(s)$, $G_{vg}(s)$ and $G_{ig}(s)$. In the present work transfer function $G_{id}(s)$ has been referred for designing the proposed control scheme. The small signal transfer function that relate the inductor current $i_l(s)$ with the variation of the duty-ratio $d(s)$ around the operation point under zero initial conditions is given by [12],
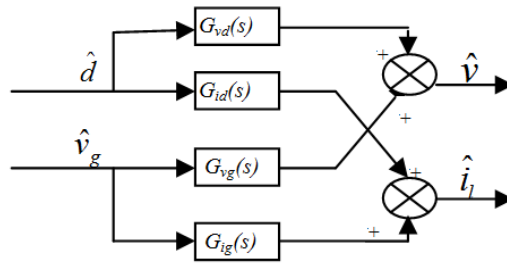

Figure 3. Transfer function model of buck converter

$$G_{id} = \frac{\hat{i}_l(s)}{\hat{d}(s)} = \frac{V}{DR_L} \times \frac{1 + sR_LC}{1 + s(L/R_L) + s^2LC} \qquad (14)$$

where, *V* is maximum output voltage, *D* is nominal duty-ratio, R_L is maximum load resistance, *L* is inductor and *C* is capacitor values. This Laplace domain transfer function has to be converted in to state space form for LQR design. The buck converter for solar PV has been designed to work in continuous conduction mode with the parameters shown in Table 1.

Table 1. Buck Converter Parameters

Vin	20.8 Volt
Vout	16.7 Volt
Pmax	36.8 Watt
Switching frequency	80 KHz
Max. inductor current ripple	10 %
Inductor	1 mH
R_L	7,55 Ohm
Cout	100 μF
D	0.8

For the parameters of buck converter mentioned in table 1, $G_{id}(s)$ is found to be,

$$G_{id} = \frac{3.4437 + (2.6 \times 10^{-6})s}{1 + (0.1324 \times 10^{-3})s + (0.1 \times 10^{-6})s^2} \qquad (15)$$

This time domain transfer function can be converted in to state space form using *tf2ss* command in MATLAB™. For equation (15), matrices *A, B, C* and *D* have been found to be,

$$A = \begin{bmatrix} -1324 & -2441 \\ 4096 & 0 \end{bmatrix}, B = \begin{bmatrix} 128 \\ 0 \end{bmatrix}, C = \begin{bmatrix} 0.2031 & 65.68 \end{bmatrix}, D = \begin{bmatrix} 0 \end{bmatrix}. \tag{16}$$

Stability of the open loop transfer function G_{id} can be checked by finding poles of the system. For the system given by equation (16), both the poles lies in the left side of the *s*-plane and the open loop system is stable as well as controllable and observable. The selection of matrices *Q* and *R* determines optimality in control system design. The matrices *Q* and *R* are called the *state* and *control* penalty matrices [13] respectively and components of *Q* and *R* matrices are chosen by trial and error [14]. If the components of *Q* are chosen large relative to those of *R*, then the overshoot will be more. On the other hand, if the components of matrix *R* are large relative to those of *Q*, then settling time will be large. In the present work, initial values of the components of matrices *Q* and *R* are chosen to be:

$$Q = \begin{bmatrix} 1 & 0 \\ 0 & 0 \end{bmatrix}, R = \begin{bmatrix} 1 \end{bmatrix}. \tag{17}$$

With above values of *Q* and *R* matrices and using command *lqr(A,B,Q,R)* gain matrix *K* has been determined. The optimal regulator for the LTI system with respect to the quadratic cost function (equation (19)) is always a linear control law. The closed loop system takes the form [13],

$$u = (A - BK)x \tag{18}$$

and the cost function takes the form,

$$J = \int_0^\infty \left(x^T Q x + (-Kx)^T R (-Kx) \right) dt$$

$$J = \int_0^\infty x^T \left(Q + K^T R x \right) x\, dt \tag{19}$$

After finding the *K* matrix, closed loop system's state space equations has to be determined as,

$$A_{closed-loop} = A - BK \tag{20}$$

$$B_{closed-loop} = B \tag{21}$$

$$C_{closed-loop} = C - DK \tag{22}$$

$$D_{closed-loop} = D \tag{23}$$

Step response of the closed loop system is then determined (Figure 4) using *step( )* command of the MATLAB™. Peak overshoot and settling time has been found to be 50.8% and 0.0054 seconds respectively. Above procedure of designing closed loop LQR system and plotting its step response has been repeated for number of times by varying value of component Q_{11} of matrix *Q* from 1 to 10000 while keeping matrix *R* same. Satisfactory step response has been found at Q_{11}= 2000 with settling time equal to 1.59 milliseconds with

0.0373 % overshoot. The optimal gain matrix has been found to be, K= [35.55   0]. Before real time implementation of the LQR based MPP tracking control system the stability of the closed loop system need to be analyzed. Bode plot (Figure 5) analysis of the closed loop system has been done which shows the infinite gain margin and phase margin of 61.6 ^{0} at gain crossover frequency of 5145 rad/sec and confirms the stability of the closed loop system.
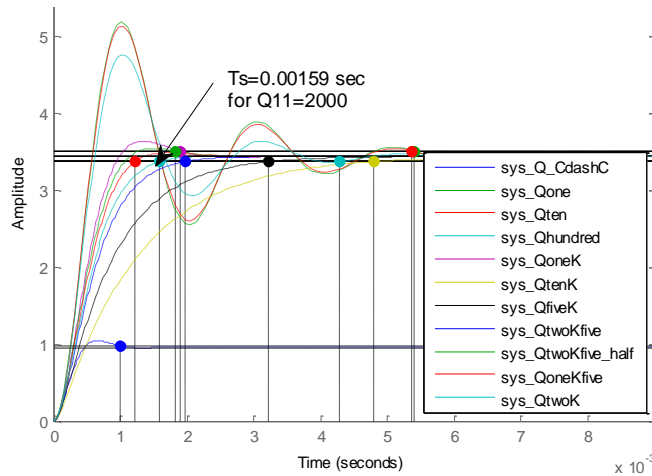

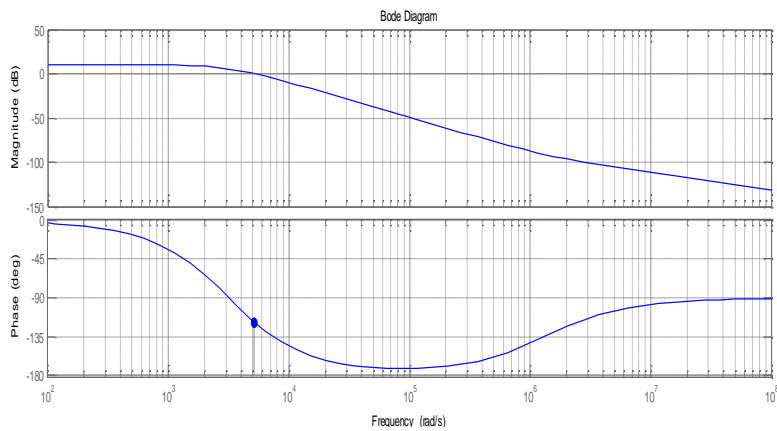**Figure 4. Step response of the closed loop system**

Figure 5. Bode plot of closed loop system with Q_{11} =2000

3. Real Time Implementation of Proposed and Existing MPPT Techniques

3.1. Hardware details

A poly-crystalline solar PV module (Vikram Solar ELV37) of specifications mentioned in Table 2, with buck converter has been used for experimental analysis of proposed and existing MPPT techniques.

Table 2. PV module parameters at standard test conditions

Short circuit current I_{sc}	2.40 A
Open circuit voltage V_{oc}	21.8 V
Current at maximum power point I_{MPP}	2.25 A
Voltage at maximum power point V_{MPP}	17 V
Number of cells in series N_s	36
Temperature coefficient of I_{sc}	0.04% /°C
Temperature coefficient of V_{oc}	-0.32%/°C
P_{max}	37W

MPPT algorithms have been designed in MATLAB™/SIMULINK™ and implemented using dSPACE™ ds1104 R & D controller board. Design specifications and the parameters of the buck converter have been mentioned in Table 1. For the proposed MPPT algorithms current and radiation sensors are needed while for other algorithms voltage and current sensors are required to be interfaced with computer system via ds1104 controller board. Also radiation and temperature sensors are needed for calculation of theoretical maximum power ($P_{max,\ theoretical}$). Voltage, current, radiation and temperature sensors have been designed and calibrated for implementation of various MPPT algorithms.

Voltage sensor is designed using voltage divider resistive network (R_p & R_v) as shown in figure 6. Output voltage is sufficiently reduced by adjusting value of the variable resistor. As per the specifications of ds1104 controller board, it accepts analogue input in the range of +/- 10 Volt.
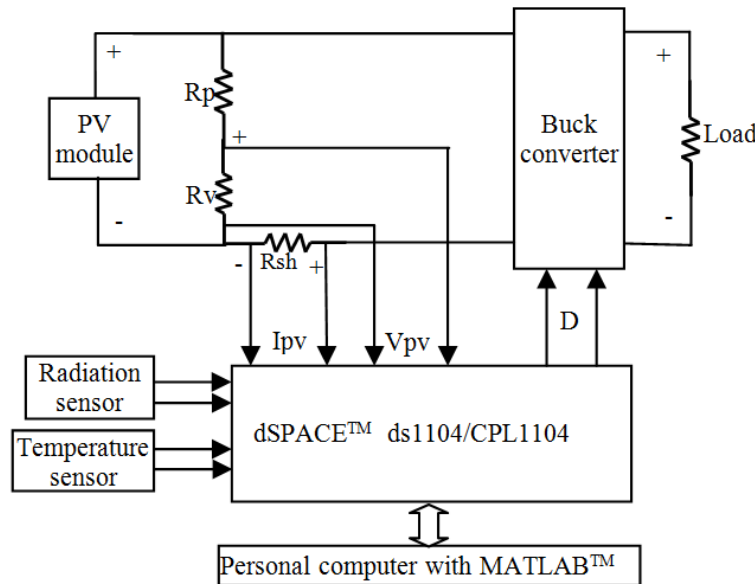

Figure 6. Hardware interfacing of proposed scheme

Current measurement has been done using low value (0.01 Ohm) shunt resistor (R_{sh}) that will output a voltage proportional to the current flowing through it. Since the shunt resistor is non-isolated caution must be exercised with its placement. A reference solar module is used for the measurement of the solar radiation. Proper calibration should be done to match the technology of the reference module with the technology of the photo-voltaic module used.

The average intensity of the solar radiation the striking on PV module was calculated by measuring the radiation level at various points on the PV panel. According to this value the output of the radiation sensor was calibrated. Extensive calibration measure has been performed on the PV module and reference module. For measurement of module temperature LM35 temperature sensor is used which gives 10mV change across output voltage per degree Celsius change in the input temperature. Two zener diodes with breakdown voltage of 10 V and a resistor of 10 K Ohm is arranged to protect ds1104 A/D converter from overvoltage. The photo snap of experimental setup and calibration of radiation sensor using reference PV module is given in Figure 7(a) and (b).
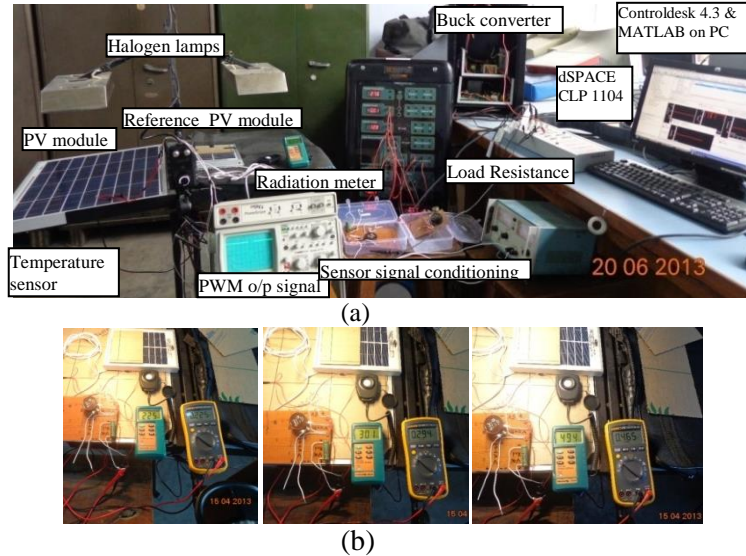

(a)

(b)

Figure 7. (a) Experimental setup and (b) Calibration of radiation sensor

3.2 Efficiency of MPPT system

The choice of the MPPT technique for a specific application is important design factor and should be based on efficiency of MPP tracker, response time, peak overshoot, static and dynamic error and sensors needed. All these parameters of MPPT system have been analyzed in the present work in order to compare various MPP tracking techniques. Efficiency is the most important parameter of an MPPT algorithm can be calculated as,

$$\eta_{MPPT} = \frac{\int_0^t P_{MPPT}(t)\,dt}{\int_0^t P_{max}(t)\,dt} \qquad (24)$$

where, P_{MPPT} presents the output power of PV system with MPPT and P_{max} is the output power at true maximum power point.

3.3 Calculation of P_{max} (theoretical)

In the present work pre-calibrated reference PV module and LM35 temperature sensor have been used to estimate the theoretical maximum power point ($P_{max, theoretical}$). Apart from short-circuit current other important characteristics of the PV module viz. open-circuit voltage

V_{oc}, fill factor *FF* and the maximum power output P_{max} are function of radiation and panel temperature [6]. The relatonship between the open-circuit voltage and radiation follows logarithmic function based on ideal diode equation and due to effect of temperature. There is exponential increase in the diode saturation current with an increase in temperature [11]. The open-circuit voltage at any given condition can be expressed by,

$$V_{oc} = \frac{V_{oc,n}}{1 + \beta \ln(S_n / S)} \left(\frac{T_n}{T}\right)^{\gamma} \tag{25}$$

where, V_{oc} and $V_{oc,n}$ are the open-circuit voltage of the PV module under the normal radiation *S* and the nominal radiation S_n , *β* is a PV module technology specific coefficient [7] and γ is the exponent considering all the non-linar effects. The values of α, *β* and *γ* can be referred from the datasheet of the solar module. Fill factor is a dimentionless term and is a measure of the deviation of the actual *I-V* characterestic from the idal one. The series and shunt resistance associated with PV modules reduce the fill factor. Expression for determination of the fill factor can be given by,

$$FF = FF_0 \left(1 - \frac{R_s}{V_{oc} / I_{sc}}\right) \tag{26}$$

where,

$$FF_0 = \frac{v_{oc} - \ln(v_{oc} + 0.72)}{1 + v_{oc}} \tag{27}$$

with, FF_0 is the fill factor of the ideal PV module without resistance effects, R_s is the series resistance, v_{oc} is the normalized value of the open-circuit voltage to the thermal voltage i.e.,

$$v_{oc} = \frac{V_{oc}}{nkT / q} \tag{28}$$

The maximum power output P_{max} can be given by,

$$P_{\max} = FF \times V_{oc} \times I_{sc}$$

$$P_{\max} = \frac{v_{oc} - \ln(v_{oc} + 0.72)}{1 + v_{oc}} \left(1 - \frac{R_s}{V_{oc} / I_{sc}}\right) \frac{V_{oc,n}}{1 + \beta \ln(S_n / S)} \left(\frac{T_n}{T}\right)^{\gamma} I_{sc,n} \left(\frac{S}{S_n}\right)^{\alpha} \tag{29}$$

An algorithm for calculation of $P_{max,theoretical}$ has been modeled in MATLAB^{TM}/SIMULINK^{TM} has been designed using equation (29). Values of *α, β* and *γ* are referred from the Vikram Solar PV module ELV37 datasheet.

3.4 Modeling and real-time simulation of MPPT algorithms

MATLAB^{TM}/SIMULINK^{TM} models of various MPPT algorithms have developed and laboratory based real time simulations have been carried out for comparing proposed and existing algorithms based on their responses for step change in the solar irradiation. Step

change in the solar radiation of the two halogen lamps was introduced using toggle switches.

In the present work static and dynamic relative error of the PV output power has been analyzed. All the MPPT control algorithms have been programmed with MATLAB^{TM} and implemented using dSPACE^{TM} ds1104 R&D controller board and CLP1104 connecter and LED panel. Four channels of analogue data input and one channel of PWM output channel have been used to interface four sensors (voltage, current, radiation and temperature sensors) and one output signal (duty-ratio). The dSPACE^{TM} system samples and converts the sensor outputs to digital signals, processes them as per program in MATLAB^{TM} and then outputs the pulse-width-modulated (PWM) signal to the driving circuit of the buck converter via PWM output channel. As per the specifications of the dSPACE^{TM} for analogue input in the range -10 V to +10 V, the SIMULINK^{TM} output is in the range -1 V to +1 V [15]. Hence proper gains for input and output signals need to be chosen. The model for implementing LQR based MPPT algorithm is given in Figure 8(a) & (b). The optimal value of the gain matrix K is given by [35.55   0] has been used to design linear quadratic regulator. PV current I_{pv} is all the time compared with current at maximum power I_{mp} value of which is determined based on solar radiation and panel temperature. One of the PWM channels of the ds1104 is used to output the 80 KHz pulses whose duty-ratio is adjusted by MPPT controller.

Models of P&O and INC MPPT have been developed with initial value of the duty-ratio of 0.8. Fuzzy based MPPT system has been designed using two input variables [8] viz. dP/dV and rate of change of dP/dV ($\Delta\, dP/dV$) given by,

$$\frac{dP}{dV}(k) = \frac{p(k) - p(k-1)}{V(k) - V(k-1)}$$

(30)

$$\Delta\left(\frac{dP}{dV}(k)\right) = \frac{dP}{dV}(k) - \frac{dP}{dV}(k-1)$$

(31)

and one output variable viz. change in duty-ratio (ΔD). Seven triangular membership functions have been assigned for input and output variables. The rule base is given in Table 3. Mamdani method of fuzzification and centroid method of defuzzification are used for real time implementation of the fuzzy MPPT algorithm.

Neural network based MPPT controller is modeled with two layer feed-forward neural network with ten sigmoid hidden neurons and designed with *nntool* of MATLAB^{TM}. The network has been trained with experimental set of input data using Levenberg-Marquardt back-propagation algorithm. A total of 7609 samples were collected from real time system out of which 5327 samples (70%) were used to train the network while remaining samples were used for validation and testing purpose. The mean square error (MSE) and regression of the NN model developed is given in Table 4. Mean squared error is the avarage squared difference between outputs and targets while regression gives the correlation between outputs and targets. A value of regression equal to 1 refers to a close relationship while 0 is for random relationship.
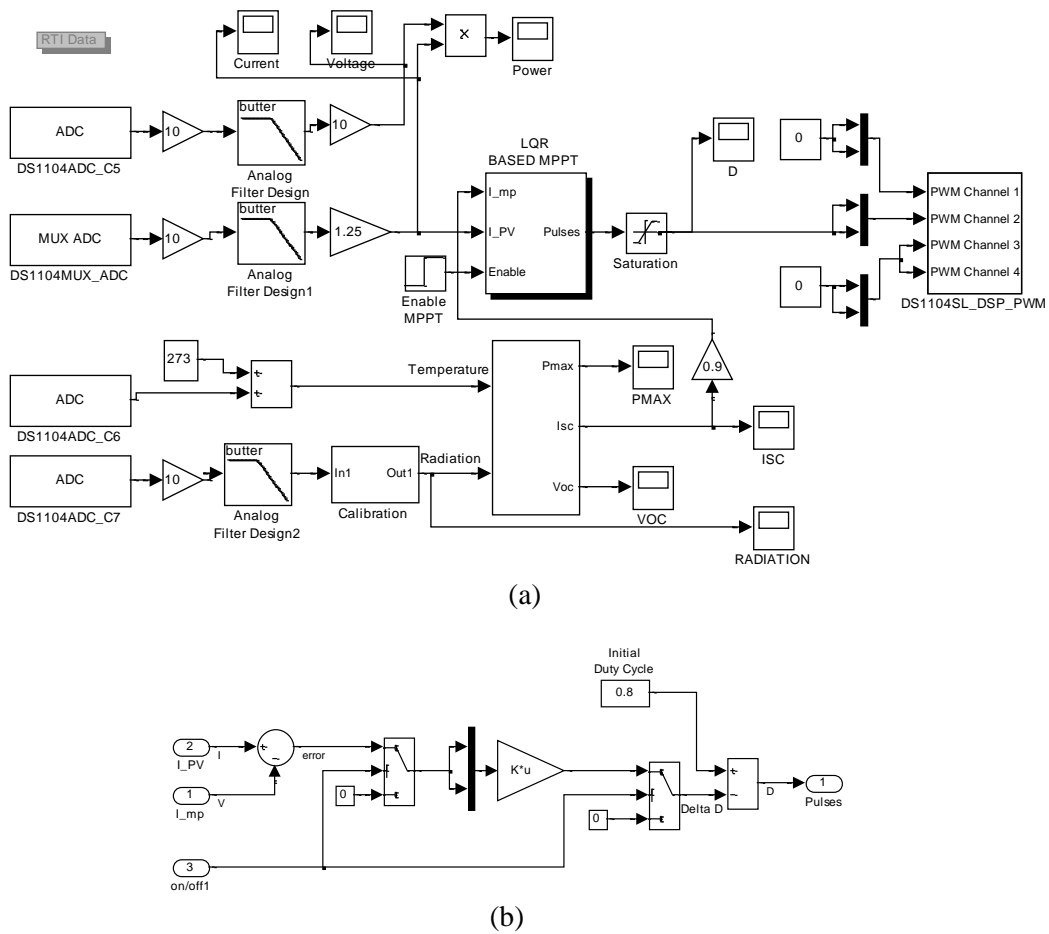
(a)

(b)

Figure 8. (a) Model of LQR based MPPT system and (b) LQR-MPPT subsystem

Table 3. Rule base for fuzzy-MPPT system

dP/dV → rate_dP/dV ↓	NB	NM	NS	ZE	PS	PM	PB
NB	ZE	ZE	NS	NM	PM	PM	PB
NM	ZE	ZE	ZE	NS	PS	PM	PB
NS	ZE	ZE	ZE	ZE	PS	PM	PB
ZE	NB	NM	NS	ZE	PS	PM	PB
PS	NB	NM	NS	ZE	ZE	ZE	ZE
PM	NB	NM	NS	PS	ZE	ZE	ZE
PB	NB	NM	NS	PM	PS	ZE	ZE

Table 4. MSE and regression values of training, validation and testing process

	Samples	MSE	Regression
Training	5327	$2.9249*10^{-9}$	$1.9088*10^{-1}$
Validation	1141	$2.8218*10^{-9}$	$1.9335*10^{-1}$
Testing	1141	$2.8890*10^{-9}$	$1.7976*10^{-1}$

In the present work the ANFIS controller has been developed with two inputs (PV current and voltage) and one output (duty-ratio). In this controller fuzzy rule base has been generated based on Sugeno inference model. The data for training kept same as that of NN based MPPT design. The *anfisedit* tool of MATLAB has been used to design the ANFIS controller with two neurons in layer 1 and 14 neurons in the fuzzification layer.

4. Results and discussions

Response of various MPPT algorithms has been shown in Figure 9(a) to (h). Variation in $P_{max}(actual)$ with respect to step change in input solar radiation intensity has been plotted along with $P_{max}(theoretical)$. Theoretical value of P_{max} has been determined based on the radiation and temperature sensor outputs. Performance of P & O MPPT method was analyzed with different fixed perturbation sizes (ΔD=0.001 to 0.1). It can be seen from the responses that the steady state oscillations have been reduced and efficiency has been increased with decrease in ΔD and satisfactory response can be achieved with ΔD=0.001, but overall MPPT efficiency is limited to around 85 %. Real time simulations have been carried out for 4-5 times under different conditions and lower and higher value of the efficiency obtained by using various MPPT techniques has been mentioned in the Table 5. Except efficiency other parameter values mentioned in the Table 5 are maximum values obtained in real time simulations. The initial offset shown in the Figure 9(a) is the difference between the theoretical P_{max} calculated (of the order of 0.04 Watt) with ambient temperature and radiation (with halogen lamps in off condition) and the actual power determined using PV voltage and current sensors. It is noted that effect of this initial offset has been ignored while the efficiency analysis for all MPPT algorithms.

Incremental conductance method of MPPT exhibit very little steady state oscillations and steady state error is almost half of that of P&O MPPT, but offers overshoot (3.35%) with response to abrupt change in the input radiation. The settling time in case of INC is large than that of P & O MPPT. It can be seen that the dynamic response has been improved as compared to the P & O MPPT.

Fuzzy logic based MPPT technique resulted in about 89 % of efficiency with lower settling time and the steady state error as compared to the INC technique of MPPT. Other artificial intelligence based techniques offered higher efficiency as mentioned in Table 5. Good balance between overshoot, steady state error and settling time can be achieved with well trained neural network based MPPT. Although the ANFIS MPPT method resulted in higher efficiency it offered much higher overshoot and settling time. All the MPPT techniques mentioned above uses voltage and current sensors for their working and calculation of power is essential for MPP tracking.

The proposed LQR based MPPT technique offered much better efficiency with less overshoot and settling time. The effect of change in sampling time of data acquisition has also been analyzed. It is seen that for larger sampling frequency the steady state error has been greatly reduced. Although parameter tuning is essential in the case of proposed LQR based MPPT technique no power calculation is required for MPP tracking.
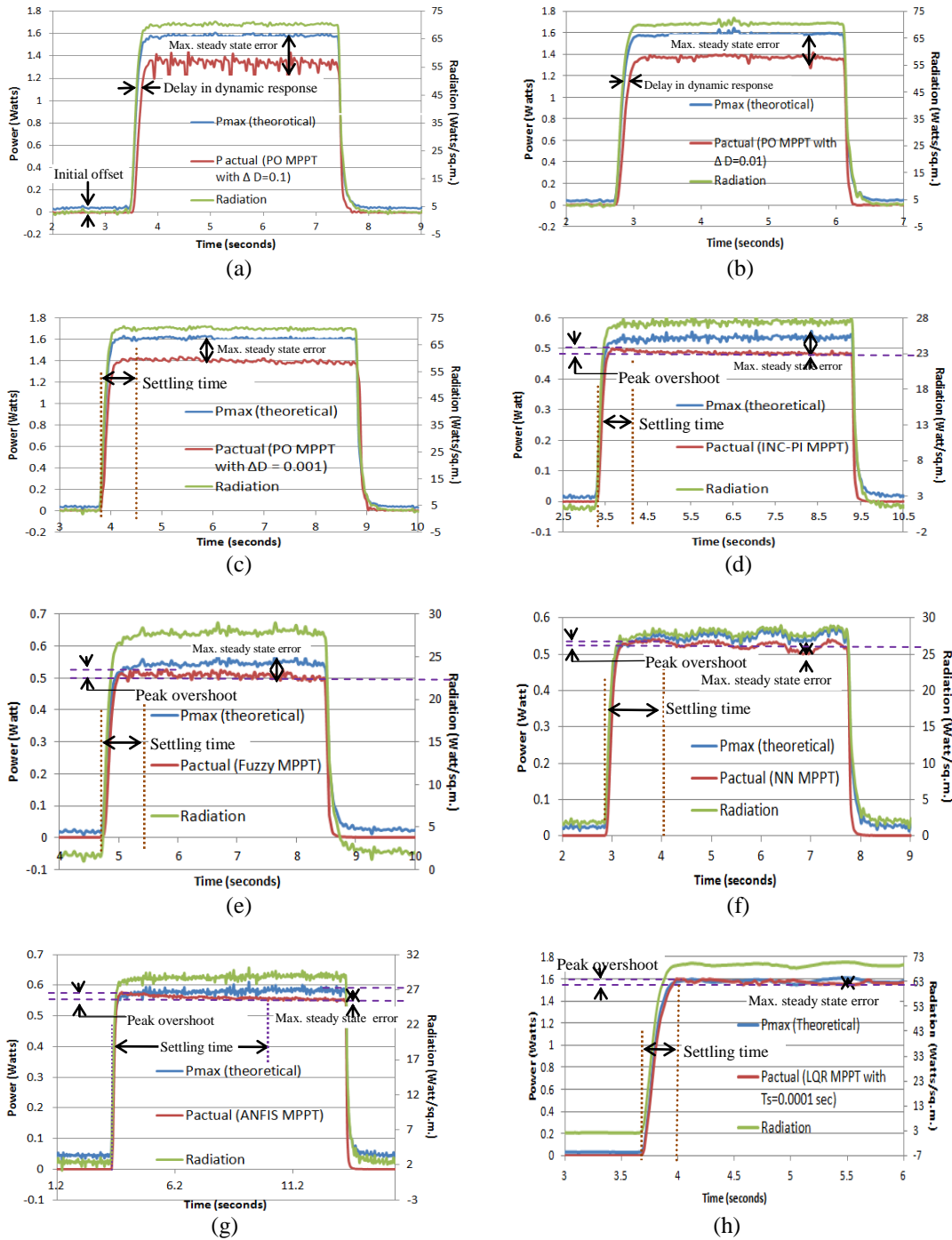
Figure 9. (a) Response of PO MPPT with *ΔD*=0.1, (b) Response of PO MPPT with *ΔD*=0.01, (c) Response of PO MPPT with *ΔD*=0.001, (d) Response of INC-PI MPPT, (e) Response of fuzzy MPPT (f) Response of NN MPPT, (g) Response of ANFIS MPPT and (h) Response of LQR based MPPT with sampling time= 0.0001 sec.

Table 5. Comparison of proposed and existing MPPT algorithms

MPPT method	Efficiency (%)	Overshoot (%)	Settling time (sec)	Delay in dynamic response (sec)	Max. Steady state error (%)	Sensors used
P & O (with ΔD=0.1)	77.60 to 79.39	No	0.48	0.06	15.14	Voltage, current
P & O (with ΔD=0.01)	81.00 to 81.60	No	0.41	0.039	12.77	Voltage, current
P & O (with ΔD=0.001)	81.23 to 84.37	No	0.40 sec	0.04	12.03	Voltage, current
INC PI	86.32 to 87.25	3.35	1.78	0.001	7.35	Voltage, current
FUZZY	85.63 to 88.88	4.32	0.472	0.039	3.63	Voltage, current
NN	87.35 to 90.10	2.185	0.6439	0.038	3.88	Voltage, current
ANFIS	87.15 to 93.31	6.56	5.35	0	0	Voltage, current
LQR T_{sample}= 0.0001 sec	90.87 to 94.78	1.389	0.53	0.0096	2.41	Current, radiation, temperature

5. Conclusions

A new LQR based optimal MPP tracking approach has been proposed to improve the performance of the conventional current feedback MPPT method. Two MPPT (LQR based and LQR tuned PI based) controllers have been designed using PV current, solar radiation and panel temperature sensors. Real time simulations of proposed and conventional MPPT algorithms have been carried out for performance comparison and validation. The experimental results show that the proposed approach can achieve better efficiency as compared to P & O, incremental conductance, fuzzy logic, neural network or ANFIS based MPPT techniques under rapidly changing solar radiations. Although the proposed approach needs three sensors, it does not require calculation of PV power as in the case of other conventional methods. Future work includes experimental implementation of proposed method for grid connected solar PV system with multilevel inverter.

Acknowledgements

References

[1] B. Subudhi and R. Pradhan, "A comparative study on maximum power point tracking techniques for photovoltaic power systems", IEEE Trans. Sustain. Ener., vol. 4, **(2013)**, pp. 89-98.
[2] T. Esram and P. Chapman, "Comparison of photovoltaic array maximum power point tracking techniques", IEEE Trans. Energy Convers., vol. 22, **(2007)**, pp. 439-449.
[3] L. Oscar and T. P. Maria, "A new MPPT method for low-power solar energy harvesting", IEEE Trans. Ind. Electron., vol. 57, **(2010)**, pp. 3129-3138.
[4] M. G. Marcelo, J. Gazoli and E. Filho, "Comprehensive approach to modeling and simulation of photovoltaic arrays", IEEE Trans. Power Electron., vol. 24, **(2009)**, pp. 1198-1208.

[5] J. S. Kumari, S. Babu and J. Yugandhar, "Design and investigation of short circuit current based maximum power point tracking for photovoltaic system", Sci. Academ. J. of Research and Reviews in Elect. and Comp. Engg., vol. 2, **(2011)**, pp. 63-68.

[6] W. Zhou, H. Yang and Z. Fang, "A novel model for photovoltaic array performance prediction", J. of Appl. Energ., vol. 84, **(2007)**, pp. 1187–1198.

[7] V. Dyk, "Long-term monitoring of photovoltaic devices", Renew. Energ. 22 **(2002)**, pp. 183–197.

[8] S. Kartika, P. Rathika and D. Devaraj, Fuzzy logic based maximum power point tracking designed for 10Kw solar photovoltaic system, J. of comp. Sci. and Manag. Research, vol. 2, **(2013)**, pp. 4121-1427.

[9] K. Ogata, "Modern Control Engineering", fourth ed., Prentice Hall, New Jersey, **(2002)**, pp. 896-910.

[10] M. Rashid, "Power Electronics Handbook", Academic Press, **(2001)**, pp. 213-214.

[11] C. Luis and S. Sivestre, "Modelling photovoltaic systems using PSpice", John Wiley & Sons Ltd., **(2002)**.

[12] R.W. Erickson and D. Macsimovic, "Fundamentals of Power Electronics", second ed., Kluwer Academic, New York, **(2001)**, pp. 464-471.

[13] R. Ismail, M.A. Ahmad and M.S. Ramli, "Speed control of buck-converter driven dc motor using LQR and PI: A comparative assessment", Proceedings of Info. Manag. and Engg., **(2009);** Kuala Lumpur, pp. 651-655.

[14] F. B. Poyen, D. Mukherjee, D. Banerjee and S. Guin, "Implementation of linear quadratic regulator for CSTR tank", Proceedings of Adv. in Electron. and Elect. Engg., **(2013)**; Bangkok, pp. 11-15.

[15] N. Quijano, K. Passino and S. Jogi, "A tutorial introduction to control systems development and implementation with dSPACE", **(2012)**.

Authors

Dnyaneshwar Sadanand Karanjkar is pursuing Ph. D. from Punjab University, Chandigarh, India and working as Head of Instrumentation Engineering Department, Institute of Petrochemical Engineering, Lonere, Maharashtra, India. He is having 18 years academic experience and published 22 research articles in journals and conferences. His areas of interests are control system, power electronics and solar photo-voltaic system.

Dr. S. Chatterji is presently with National Institute of Technical Teaches' Training & Research, Chandigarh, India as Professor and Head of Electrical Engineering Department. He is having 38 years academic and industrial experience. He has published three books in the area of power electronics and industrial control and more than 80 research articles in reputed journals and conferences. His areas of interest are Power Electronics, Electrical Power, Microprocessor/Microcontrollers and Soft Computing Techniques.

Dr. Amod Kumar is with Central Scientific Instruments Organization, Chandigarh, India as Scientist 'G' and Vertical In-charge. He is having research experience of 33 years and published 30 journal and 12 conference papers. He has supervised large number of R & D projects in the area of diagnostic and therapeutic instruments and control systems. His areas of interest include control system, bio-medical instrumentation and digital signal processing.